Phytopathology Research

RESEARCH

Open Access

The 40S ribosomal protein SA-2 inhibits citrus yellow vein clearing virus infection in Eureka lemon via activating jasmonic acid and photosynthetic pathways

Ping Liao[1], Mengyang Huangfu[1], Dongdong Ding[1], Xue Dan[1], Li Chen[2], Binghai Lou[3*] and Yan Zhou[1*]

Abstract

The 40S ribosomal protein SA (RPSA) functions as an important regulatory factor in plant resistance to abiotic stresses. However, the role of RPSA in response to plant virus infection is poorly understood. Citrus yellow vein clearing virus (CYVCV) has a significantly negative impact on citrus production, and its coat protein (CP) is involved in viral pathogenicity. In this study, we revealed the interaction of CP with Eureka lemon 40S RPSA (ClRPSA-2) in the nucleus, membrane, and endoplasmic reticulum of *Nicotiana benthamiana*. Further experiments demonstrated that the ClRPSA-2 N-terminal conserved region (amino acids 22—122) was involved in the interaction with CP, and the *ClRPSA-2* expression in young Eureka lemon leaves significantly reduced. Transient expression of *ClRPSA-2* triggered the expression of jasmonic acid (JA), photosynthetic pathway- and resistance-related genes, as well as increased the JA content and maximum photochemical efficiency (*Fv/Fm*) in lemon. Furthermore, ClRPSA-2 negatively regulated CYVCV resistance in plants, which induced resistance to other citrus viruses. These findings enhance our understanding of the interaction between CYVCV and citrus plants and provide a basis for future research on resistance breeding of citrus.

Keywords Citrus yellow vein clearing virus, Coat protein, Disease resistance, 40S ribosomal protein

Background

Ribosomes have important functions in cellular processes such as transcription, cell cycle, mRNA processing, and DNA repair. Plant ribosomal proteins (RPs) have been divided into two major groups, 60S and 40S subunit RPs, which are the basic translational machines of living cells (Chang et al. 2005; Xiong et al. 2021). Several plant 40S RPs contribute to plant immunity by participating in plant responses to viruses. For example, *RPS6s* and *GmRPS8* negatively regulate plant resistance to cucumber mosaic virus (CMV), turnip mosaic virus, potato virus A, tomato spotted wilt virus, potato virus X, and soybean mosaic virus (SMV) (Rajamäki et al. 2017; Helderman et al. 2022; Hu et al. 2023). In contrast, *CsRPS21* positively regulates *Nicotiana benthamiana* resistance

*Correspondence:
Binghai Lou
binghai.lou@hotmail.com
Yan Zhou
zybook1@163.com
[1] Integrative Science Center of Germplasm Creation in Western China (CHONGQING) Science City, National Citrus Engineering and Technology Research Center, Citrus Research Institute, Southwest University, Chongqing 400712, China
[2] Chongqing Wanzhou Distric Economic Crop Development Center, Chongqing 404100, China
[3] Guangxi Key Laboratory of Germplasm Innovation and Utilization of Specialty Commercial Crops in North Guangxi, Guangxi Academy of Specialty Crops, Guilin 541004, Guangxi, China

to cucurbit chlorotic yellows virus (CCYV) (Yang et al. 2021).

Citrus is an important fruit crop and has been cultivated in China for more than 4000 years. Currently, China is the world's largest citrus producer, with a production of 6003.89 million tons of citrus fruit in an area of 303.35 million hectares in 2022 (National Bureau of Statistics 2023). Citrus yellow vein clearing virus (CYVCV) is a devastating virus in citrus, causing significant economic losses in Pakistan, India, Turkey, China, Iran, South Korea, and the United States (Liu et al. 2019; Abrahamian et al. 2024; Sun and Yokomi 2024). Although CYVCV is not seed-transmissible, it can rapidly spread through CYVCV-infected budwood, contaminated tools, and some Hemipteran insect species (Zhang et al. 2019a, b; Liu et al. 2020; Maghsoudi et al. 2023).

As members of the genus *Mandarivirus*, CYVCV is closely related to Indian citrus ring spot virus; however, there are significant serological differences between the two viruses (Meena and Baranwal 2020). Some host proteins can interact with the coat protein (CP, a pathogenic factor) of CYVCV and regulate the host defense response against CYVCV infection (Bin et al. 2022; Wang et al. 2023; Liao et al. 2024). Zeng et al. (2023) revealed the interaction between Eureka lemon 40S ribosomal protein S9-2 (ClRPS9-2) and the CYVCV CP, and ClRPS9-2 can reduce CP accumulation and inhibit the RNA silencing activity of CP. In addition, the Eureka lemon 40S ribosomal protein, ClRPSA-2, interacts with the CP in yeast (Zeng et al. 2023).

The 40S ribosomal protein SA (RPSA) is a multifunctional protein that participates in tumor invasion (Fatehullah et al. 2010; Ould-Abeih et al. 2012) and acts as a membrane receptor for viruses (Tio et al. 2005; Malygin et al. 2009). 40S ribosomal protein SA-like protein (CaSLP) improves *Pseudomonas syringae* pv. *tomato* (*Pst*) DC3000 tolerance in pepper and *Arabidopsis* (Zhang et al. 2023). However, the function of RPSA in plant viral disease resistance remains unclear.

Therefore, we aimed to determine the function of ClRPSA-2 in plant disease resistance in this study, and found that ClRPSA-2 interacted with the CYVCV CP and inhibited CP accumulation by triggering the jasmonic acid (JA) and photosynthesis pathways. Furthermore, transient expression of *ClRPSA-2* enhanced citrus resistance to CYVCV and other viruses tested.

Results

Characterization of ClRPSA-2

The SMART online assay showed that ClRPSA-2 consists of 316 amino acids (aa) and contains two conserved rbosomal_S2 domains (Additional file 1: Figure S1a). To evaluate RPSA-2 conservation in plants, homologous RPSA-2 sequences from *Citrus*, *Citrus*-related genera, and other non-*Citrus* genera were analyzed. We found that the similarity of these homologous RPSA-2 sequences ranged from 64.94% to 100.00%. The similarity between RPSA-2 from *Citrus* and *Citrus*-related genera was over 91.88% (Additional file 2: Table S1). In addition, all RPSA-2 sequences from *Citrus* and *Citrus*-related genera clustered together in the phylogenetic tree, which was generated using the neighbor-joining method (Additional file 1: Figure S1b). As shown in Additional file 2: Table S2, ClRPSA-2 contains nucleotide-binding sites such as MYB, MYC, ABRE, and G-box, which are closely related to light and MeJA responses, and confer stress resistance.

CYVCV-CP interacts with ClRPSA-2

To confirm the interactions between CP and ClRPSA-2, BD:CP and AD:ClRPSA-2 were used in the yeast two-hybrid (Y2H) assay. Y2H Gold competent cells harboring BD:CP and AD:ClRPSA-2 produced blue clones on SD/-Trp/-Leu/-His/-Ade/AbA/X-α-Gal medium (Fig. 1a). Subsequently, co-immunoprecipitation (Co-IP) was used to analyze the putative CP/ClRPSA-2 interaction in vivo. At 2 days post infiltration (dpi), the results suggested that CP-GFP co-immunoprecipitated with ClRPSA-2-His but not with GFP (Fig. 1b). In the luciferase complementation imaging (LCI) assay, *CP* and *RPSA-2* were ligated into PHNL:P14 and PCCL:P9 vectors to express CP and RPSA-2, respectively, with an N-terminal split-luciferase tag in *N. benthamiana*. Luminescence was observed in *N. benthamiana* leaves co-expressing CP/RPSA-2 or CP/TGBp1 (positive control) at 2 dpi; however, no luminescence signal was detected in the negative control (Fig. 1c). Finally, pSPYCE:CP was agro-infiltrated with pSPYNE:ClRPSA-2 into *N. benthamiana*. Two days later, yellow fluorescence was observed in the nucleus and membrane of *N. benthamiana* leaf cells (Fig. 1d). No fluorescence was observed in *N. benthamiana* leaves co-infiltrated with pSPYCE:CP and pSPYNE or pSPYNE:ClRPSA-2 and pSPYCE as negative controls. These results confirmed that CP directly interacts with ClRPSA-2 and that the nucleus and membrane are the interaction sites.

To clarify the key segments of the ClRPSA-2 interaction with CP, the Y2H assay was conducted using BD:CP and prey vectors that carrying four ClRPSA-2 deleted constructs. The results indicated that the yeast cells transformed with BD:CP/AD:ClRPSA-$2_{22—122}$ produced blue colonies on the SD/-Trp/-Leu/-His/-Ade/AbA/X-α-Gal selective medium (Fig. 1e, f). Furthermore, the bimolecular fluorescence complementation (BiFC) and LCI assays also suggested that ClRPSA-$2_{22—122aa}$ could interact with CP (Fig. 1g, h).

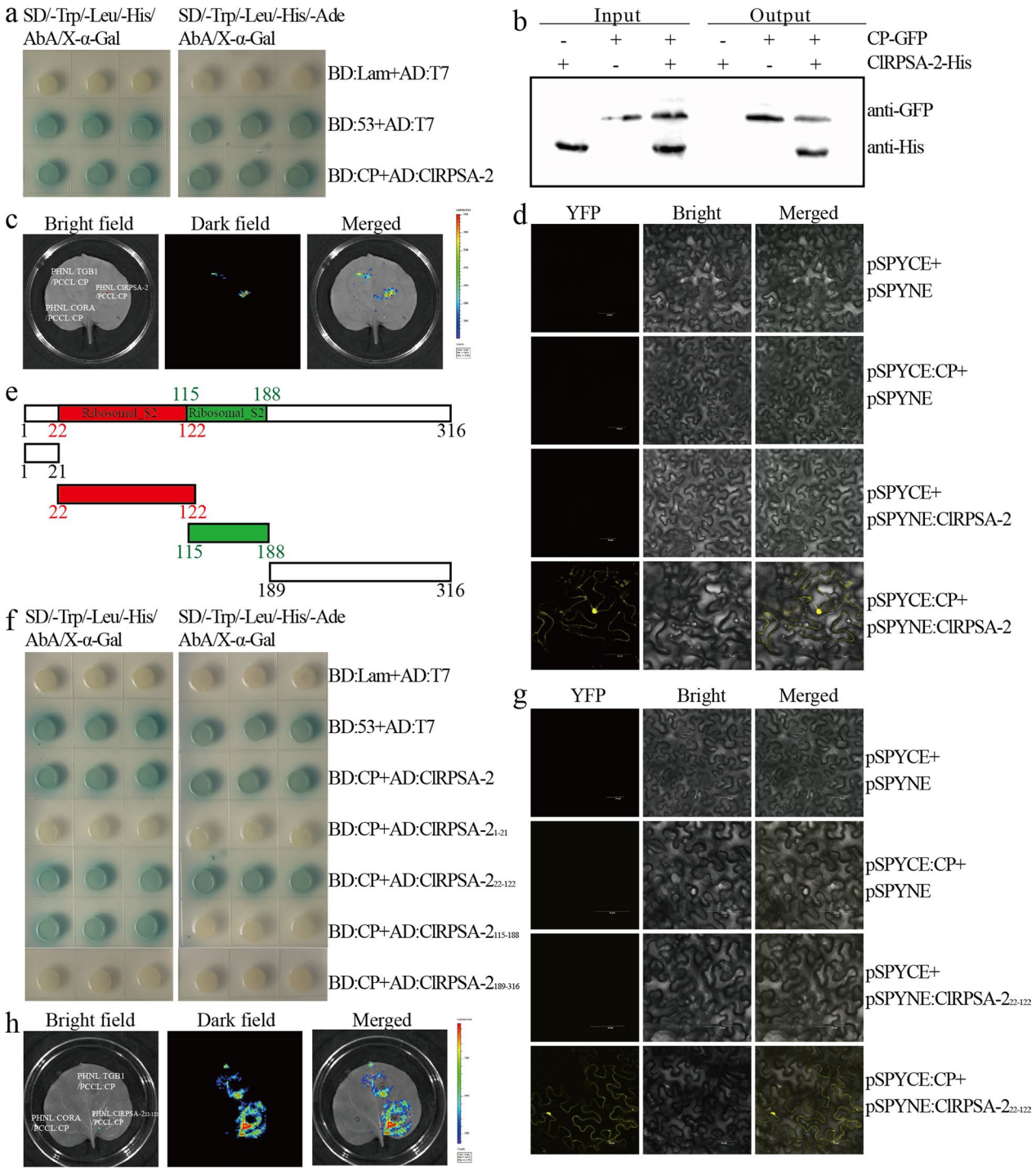

Fig. 1 Interaction between CP and ClRPSA-2 in vivo. **a** Yeast-two hybrid (Y2H) assay showed interaction between CP and ClRPSA-2. BD:53 + AD:T7, positive control, BD:Lam + AD:T7, negative control. **b** Co-immunoprecipitation assay showed that CP interacts with ClRPSA-2. Input is the positive control group, representing the detection of the target protein in the extracted total protein, and output represents the protein detection after immunoprecipitation. **c** Firefly luciferase complementation imaging (LCI) assay was used to illustrate the interaction relationship between CP and ClRPSA-2. PHNL:TGB1 + PCCL:CP, positive control, PHNL:CORA + PCCL:CP, negative control. **d** Bimolecular fluorescence complementation (BiFC) assay showed that CP and ClRPSA-2 interacted at the cell membrane and nucleus. pSPYCE + pSPYNE, pSPYCE:CP + pSPYNE, and pSPYCE + pSPYNE:ClRPSA-2 were used as negative controls. Scale bars: 50 μm. **e** Schematic representation of a truncated mutant of ClRPSA-2. **f** The interaction between CP and the ClRPSA-2 truncation mutant was analyzed by Y2H assay. **g**, **h** BiFC and LCI assays proved ClRPSA-$2_{22–122aa}$ (aa residues 22–122) interacts with CP

The interaction between CP and RPSA-2 is conserved

To clarify whether the interactions between CP and RPSA-2 were conserved in other hosts, Y2H and LCI assays were performed to validate the interaction between CP and homologous RPSA2 (CsRPSA-2, CcRPSA-2, ChRPSA-2, and NtRPSA-2). Both the Y2H and LCI assay results indicated that CsRPSA-2, CcRPSA-2, ChRPSA-2, and NtRPSA-2 could interact with CP (Fig. 2), confirming that the interaction between CP and RPSA-2 s may be conserved across species.

Distribution of ClRPSA-2 in cells

To understand the distribution of ClRPSA-2 in plant cells, the nucleotide sequence of *ClRPSA-2* was analyzed using the Cell-PLoc 2.0 software. It was predicted that ClRPSA-2 may be distributed in the cell membrane and nucleus. Subsequently, ClRPSA-2 was co-expressed with mCherry-H2B, mCherry-HDEL, and mCherry-PIP2A in *N. benthamiana*, respectively, using the pCHF3-GFP vector. Laser-scanning confocal microscopy at 2 dpi revealed that ClRPSA-2 existed in the nucleus, cell membrane, and endoplasmic reticulum (Fig. 3a–c). In addition, the subcellular localization of ClRPSA-2 did not change in the presence of CP (Fig. 3d).

CP enhances the expression of *ClRPSA-2*

To determine the effect of *CP* on *RPSA-2* expression, CP was expressed in young Eureka lemon leaves. Western blotting (WB) revealed that CP was expressed at 3 dpi (Additional file 1: Figure S2a). Real-time quantitative PCR (RT-qPCR) confirmed *CP* expression at 3–12 dpi (Additional file 1: Figure S2b). *ClRPSA-2* expression was significantly up-regulated at 3 dpi and peaked at 6 dpi (4.19-fold; Additional file 1: Figure S2c).

ClRPSA-2 negatively regulates CP expression

To reveal the role of ClRPSA-2 in CP expression in plants, *ClRPSA-2* was expressed in young Eureka lemon leaves using the pNmGFPer vector. The WB assay showed that ClRPSA-2 was expressed at 3 dpi and RT-qPCR revealed that *ClRPSA-2* expression peaked at 6 dpi (4.05-fold, Fig. 4a, b). At 3 dpi, pNmGFPer:CP was re-infiltrated in the infiltrated patches. At 3 and 5 days post-re-infiltration with pNmGFPer:CP, *CP* expression was 20.27% and 26.46% of the control, respectively (Fig. 4c); WB results also confirmed that CP expression was inhibited by transient *ClRPSA-2* expression (Fig. 4d). Furthermore, the truncated mutants (pNmGFPer:ClRPSA-$2_{1—21}$, pNmGFPer:ClRPSA-$2_{22—122}$,

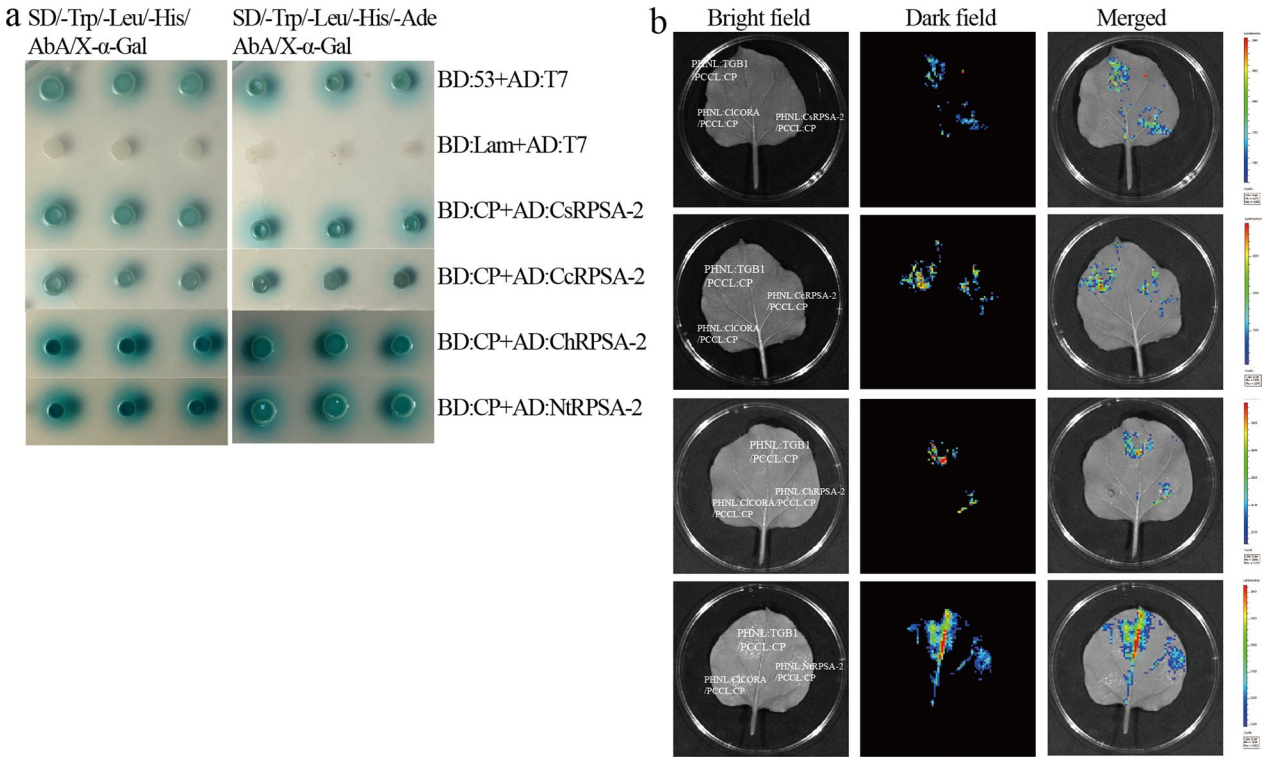

Fig. 2 The interaction between CP and RPSA-2 s. **a** Yeast-two hybrid assay showed interaction between CP and RPSA-2 s. BD:53 + AD:T7, positive control; BD:Lam + AD:T7, negative control. **b** Firefly luciferase complementation imaging assay was used to illustrate the interaction relationship between CP and RPSA-2s. PHNL:TGB1 + PCCL:CP, positive control, PHNL:CORA + PCCL:CP, negative control. CsRPSA-2 from *Citrus sinensis*, CcRPSA-2 from *C. clementina*, ChRPSA-2 from *C. hongheensis*, and NtRPSA-2 from *Nicotiana tabacum*

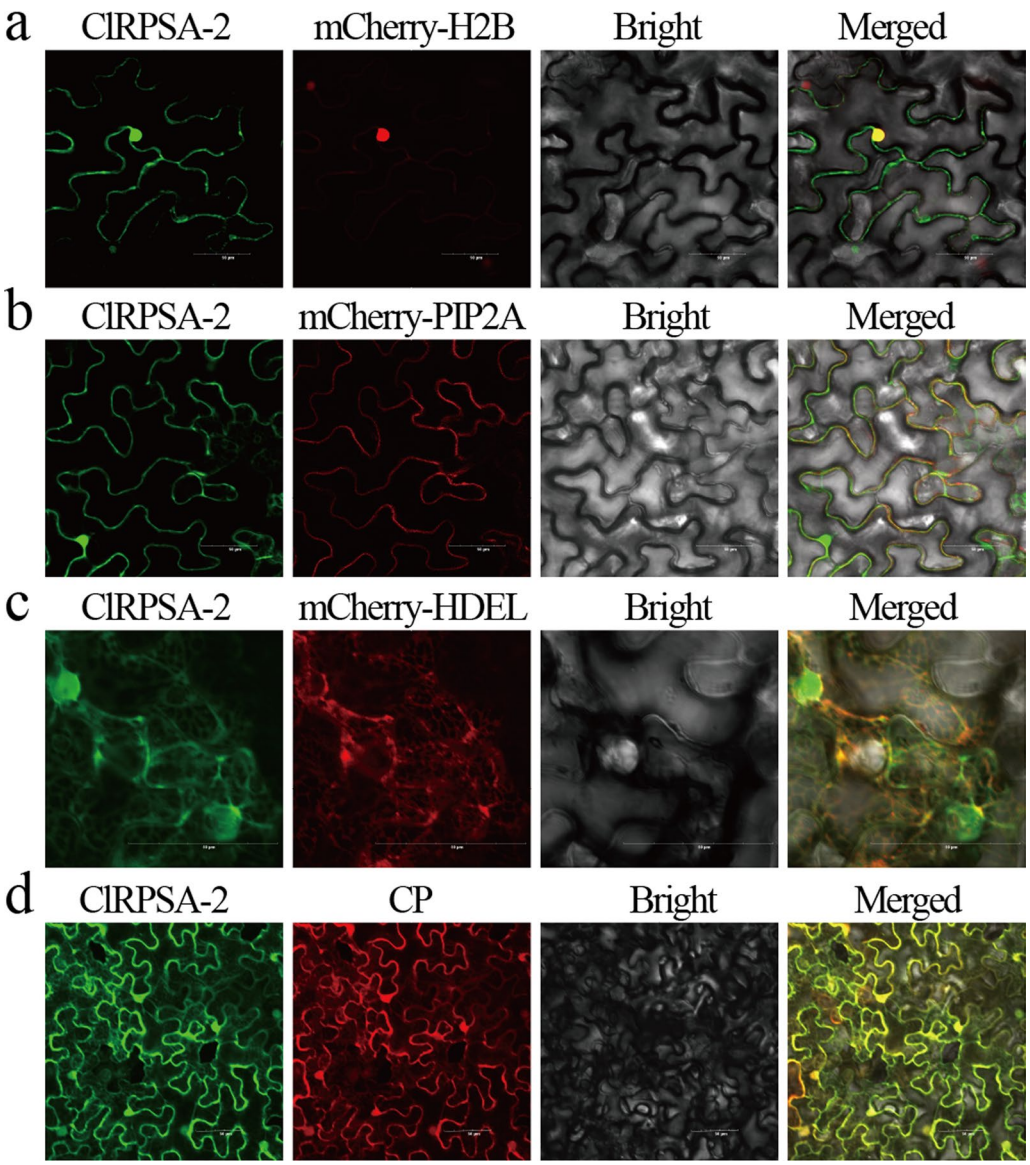

Fig. 3 Subcellular localization of ClRPSA-2 in *Nicotiana benthamiana* cells. **a**–**c** ClRPSA-2 was localized to the nucleus, cell membrane, and endoplasmic reticulum (ER). mCherry-H2B, mCherry-PIP2A, and mCherry-HDEL were used as nuclear, cell membrane, and ER markers, respectively. **d** CP co-localized with ClRPSA-2 in the nucleus, cell membrane, and ER. Scale bars: 50 μm

and pNmGFPer:ClRPSA-$2_{123—316}$) were transiently expressed in young Eureka lemon leaves. Three days later, the truncated ClRPSA-2 mutants were expressed, as confirmed by WB (Fig. 4e). Simultaneously, pNmGFPer:CP was re-infiltrated into infiltrated leaves, as described above. At 3 days post-re-infiltration with pNmGFPer:CP, RT-qPCR, and WB suggested that ClRPSA-$2_{22–122}$ inhibited CP expression (23.00%, Fig. 4f, g).

To further clarify the relationship between ClRPSA-2 and CP, *ClRPSA-2* was silenced by using the tobacco rattle virus (TRV) vector. From 3 to 12 dpi, in young *ClRPSA-2*-silenced Eureka lemon leaves, *ClRPSA-2* was down-regulated and was lowest at 6 dpi (44.76%, Additional file 1: Figure S3a). Three days later, an *Agrobacterium* culture containing pNmGFPer:CP was re-infiltrated into the above-mentioned infiltrated leaves. At 5 dpi, RT-qPCR suggested that *CP* expression in the *ClRPSA-2*-silenced leaves was 3.30-fold of the control. WB confirmed the results observed in RT-qPCR amplification (Additional file 1: Figure S3b, c). Overall, these results demonstrate that ClRPSA-2 negatively regulates CP expression in Eureka lemon.

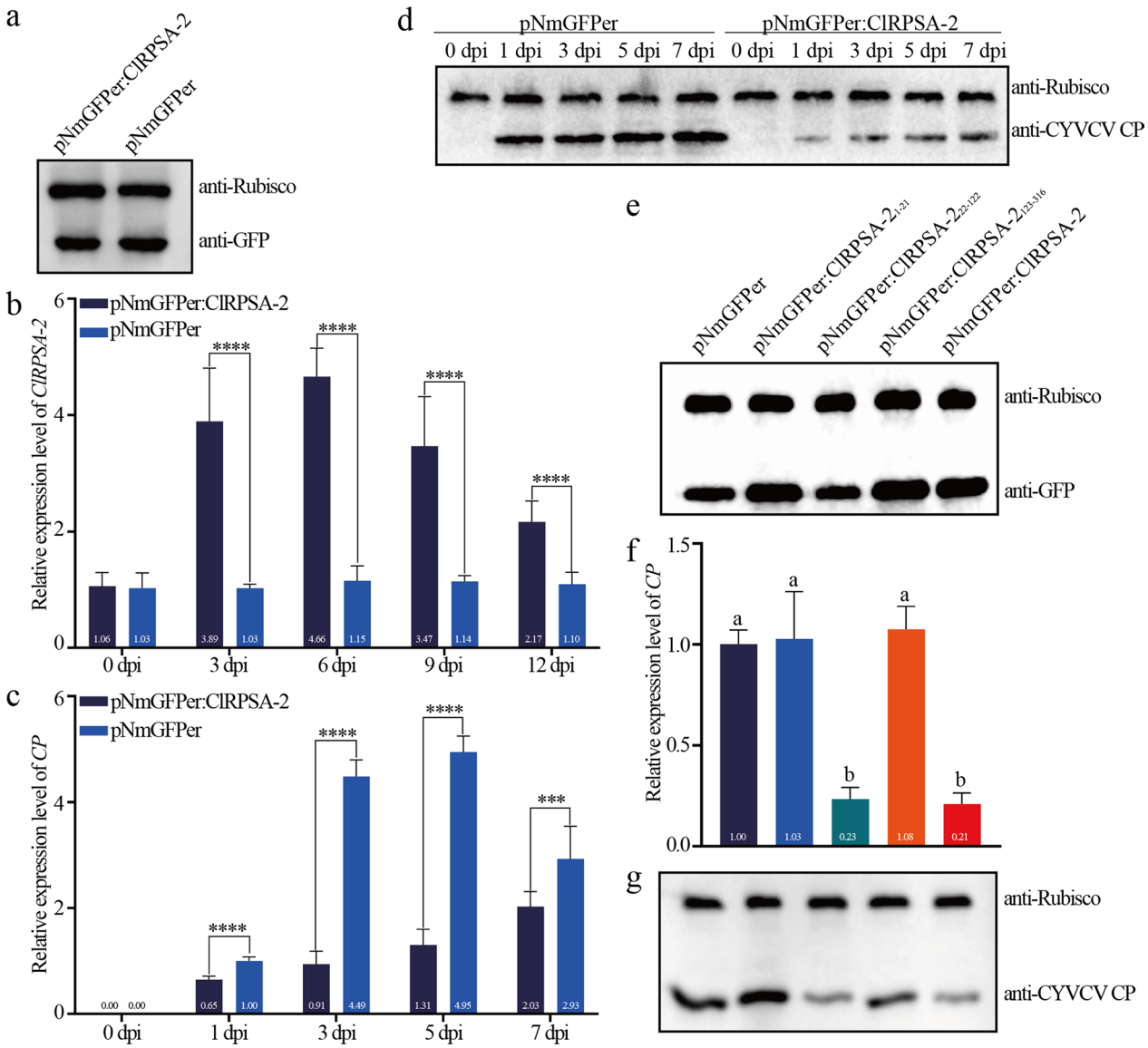

Fig. 4 *ClRPSA-2* negatively regulates CP expression. **a** Western blotting (WB) analysis was used to detect ClRPSA-2 expression at 3 days post infiltration (dpi). An anti-GFP antibody was used. **b** The relative expression level of *ClRPSA-2* was detected by real-time quantitative PCR analysis (RT-qPCR). *Actin* was an internal reference gene, *t*-test, data are mean ± SD, **** $P < 0.0001$. **c**, **d** RT-qPCR and WB analysis were used to detect CP expression. Anti-CYVCV CP antibody was used for WB analysis; *Actin* was an internal reference gene for RT-qPCR analysis, *t*-test, data are mean ± SD, $n = 9$, *** $P < 0.001$, **** $P < 0.0001$. **e** WB analysis detected ClRPSA-2 segments expression. **f**, **g** RT-qPCR and WB analysis detected CP expression in ClRPSA-2 segments expression Eureka lemon leaves. *Actin* was an internal reference gene, one-way ANOVA test at 0.05 level ($n = 9$), data are mean ± SD; An anti-CYVCV CP antibody was used for WB analysis

ClRPSA-2 triggers jasmonic acid and photosynthetic pathway expression

At 6 dpi, resistance-related genes (*NPR1*, *PR4*, *EDS1*, *R*, *UEP1*, *HIN1*, and *PAL*) were significantly up-regulated by transient *ClRPSA-2* expression and down-regulated by *ClRPSA-2* silencing (Additional file 1: Figure S4a, b). In addition, the plant disease resistance-related enzyme, phenylalanine ammonia lyase (PAL), increased (2.22-fold) after transient expression of *ClRPSA-2* (Additional file 1: Figure S4c). Motif distribution analysis showed that ClRPSA-2 contains MYC, MYB, and G-box motifs closely related to MeJA and light response. To further clarify the reasons for CP inhibition by *ClRPSA-2*, JA- and photosynthetic-related gene expression was quantified at 6 dpi in young Eureka lemon leaves where the *ClRPSA-2* gene was transiently expressed or silenced.

As shown in Fig. 5a, b, transient *ClRPSA-2* expression significantly up-regulated JA- (*MYC2*, *AOC*, *AOS*, *LOX3*, and *JAR1*) and photosynthesis (*ABC10*, *HEMG*, *CHLH*, and *CLH*) -related genes. Furthermore, *ClRPSA-2* silencing in young Eureka lemon leaves down-regulated JA- (*MYC2*, *AOC*, *AOS*, *LOX3*, and *JAR1*) and photosynthesis (*HEMA*, *ABC10*, *HEMG*, *CHLH*, *CHLI*, and *CLH*) -related genes (Additional file 1: Figure S5). In addition, we found that transient expression of *ClRPSA-2* increased the JA content (2.93-fold) and enhanced the *Fv*/*Fm* (1.45-fold) in the infiltrated leaves, while these parameters decreased by 46.57% and 20.00% in *ClRPSA-2*-silenced leaves, respectively (Fig. 5c, d). These findings suggest that ClRPSA-2 may activate plant resistance by inhibiting CP expression via JA and photosynthetic pathway activation.

To confirm the effect of ClRPSA-2 and CP on JA pathway activation, *ClRPSA-2* and *ClRPSA-2*+*CP* were transiently expressed in young Eureka lemon leaves, respectively. At 6 dpi, the JA content, *Fv*/*Fm*, and JA- and photosynthesis-related genes expression were tested. Compared with the control (Eureka lemon leaves expressing *ClRPSA-2* alone), co-expressed *ClRPSA-2*+*CP* significantly enhanced the JA content (1.52-fold), *Fv*/*Fm* (1.20-fold), and JA-related genes (*MYC2*, *LOX3*, and *JAR1*), and photosynthesis-related genes (*HEMA*, *HEMG*, *CHLH*, and *CLH*) expression (Fig. 5e–h). Compared with expressed *CP* alone, co-expressed *ClRPSA-2*+*CP* significantly reduced *CP* expression (45.54%, Fig. 5i); the WB assay obtained similar results (Fig. 5j). These findings indicated that the interaction between ClRPSA-2 and CP may induce the JA and photosynthetic pathways and inhibit CP expression.

ClRPSA-2 positively regulates Eureka lemon anti-CYVCV defense

To assess the function of ClRPSA-2 during CYVCV infection, pLGN:ClRPSA-2 and pLGN:ClRPSA-2-KO were constructed to establish the Eureka lemon hairy root *ClRPSA-2* transformation system. Sixty days later, the transformation of the hairy roots was characterized, and positive samples were used in subsequent experiments (Additional file 2: Table S3). As shown in Fig. 6a, the CYVCV titers in *ClRPSA-2* over-expressed and *ClRPSA-2*-silenced transgenic hairy roots were 37.00% and 3.40-fold those of the control, respectively. Compared with the pLGN control, resistance- (*NPR1*, *PR4*, *EDS1*, *UEP1*, *HIN1*, and *PAL*) and JA- (*MYC2*, *AOC*, *AOS*, *LOX3*, and *JAR1*) -related genes were significantly up-regulated by *ClRPSA-2* over-expression, whereas most of the genes were down-regulated by *ClRPSA-2*-silencing (Fig. 6b, c). In *ClRPSA-2* over-expressed transgenic hairy roots, the PAL and JA content was 2.11- and 2.58-fold that of the control, and *ClRPSA-2*-silencing resulted in a 47.09% and 25.23% reduction in PAL and JA content, respectively (Fig. 6d, e). These results further indicate that *ClRPSA-2* is a resistance-related gene involved in CYVCV infection inhibition via JA pathway activation.

Methyl jasmonate (MeJA) and JA inhibitor salicylhydroxamic acid (SHAM) treatments affect CYVCV accumulation through the JA signaling pathway

To further clarify whether the JA signaling pathway affects CYVCV accumulation, MeJA and SHAM solutions were sprayed on virus-free and CYVCV-infected Eureka lemon plants. In virus-free Eureka lemon plants, MeJA treatment up-regulated the expression of JA-related genes (*MYC2*, *AOC*, *AOS*, *LOX3*, and *JAR1*) and the accumulation of endogenous JA (1.96-fold); the opposite was observed in the SHAM-treated virus-free Eureka lemon plants (Fig. 7a, b). As shown in Fig. 7c, d, the CYVCV titer was reduced by exogenous MeJA treatment and increased by SHAM treatment.

ClRPSA-2 positively regulates broad-spectrum resistance to citrus viruses

To determine the resistance function of *ClRPSA-2* in other citrus viruses, *ClRPSA-2* was transiently expressed or silenced in citrus psorosis virus (CPV)-, citrus tristeza virus (CTV)-, citrus chlorotic dwarf-associated virus (CCDaV)-, and citrus tatter-leaf virus (CTLV)-infected young Eureka lemon leaves. At 6 dpi, RT-qPCR revealed that transient *ClRPSA-2* expression reduced CPV, CTV, CCDaV, and CTLV titers by 78.43%, 69.23%, 27.45%,

(See figure on next page.)

Fig. 5 *ClRPSA-2* triggers jasmonic acid (JA) and photosynthetic pathway expression. **a**, **b** Relative expression level of JA- and photosynthesis-related genes in *ClRPSA-2* transiently expressed Eureka lemon leaves. *Actin* was an internal reference gene, *t*-test, data are mean ± SD, $n = 9$, ** $P < 0.01$, *** $P < 0.001$, **** $P < 0.0001$. **c**, **d** The JA content and F_v/F_m in the *ClRPSA-2* transient expressed and silenced Eureka lemon leaves. *t*-test, data are mean ± SD, n = 5, * $P < 0.05$, *** $P < 0.001$, **** $P < 0.0001$. **e**, **f** The JA content and F_v/F_m in *ClRPSA-2* and *ClRPSA-2*+*CP* transiently expressed Eureka lemon leaves. T-test, data are mean ± SD, $n = 5$, *$P < 0.05$, ***$P < 0.001$. **g**, **h** Relative expression level of JA- and photosynthesis-related genes in *ClRPSA-2* and *ClRPSA-2*+*CP* transiently expressed Eureka lemon leaves. *Actin* was an internal reference gene, t-test, data are mean ± SD, $n = 9$, ** $P < 0.01$, *** $P < 0.001$, **** $P < 0.0001$. **i** Relative expression level of *CP* in *CP* and *ClRPSA-2*+*CP* transiently expressed Eureka lemon leaves. *Actin* was an internal reference gene, t-test, data are mean ± SD, $n = 9$, **** $P < 0.0001$. **j** Western blotting was used to detect the accumulation of CP with anti-CYVCV CP antibody

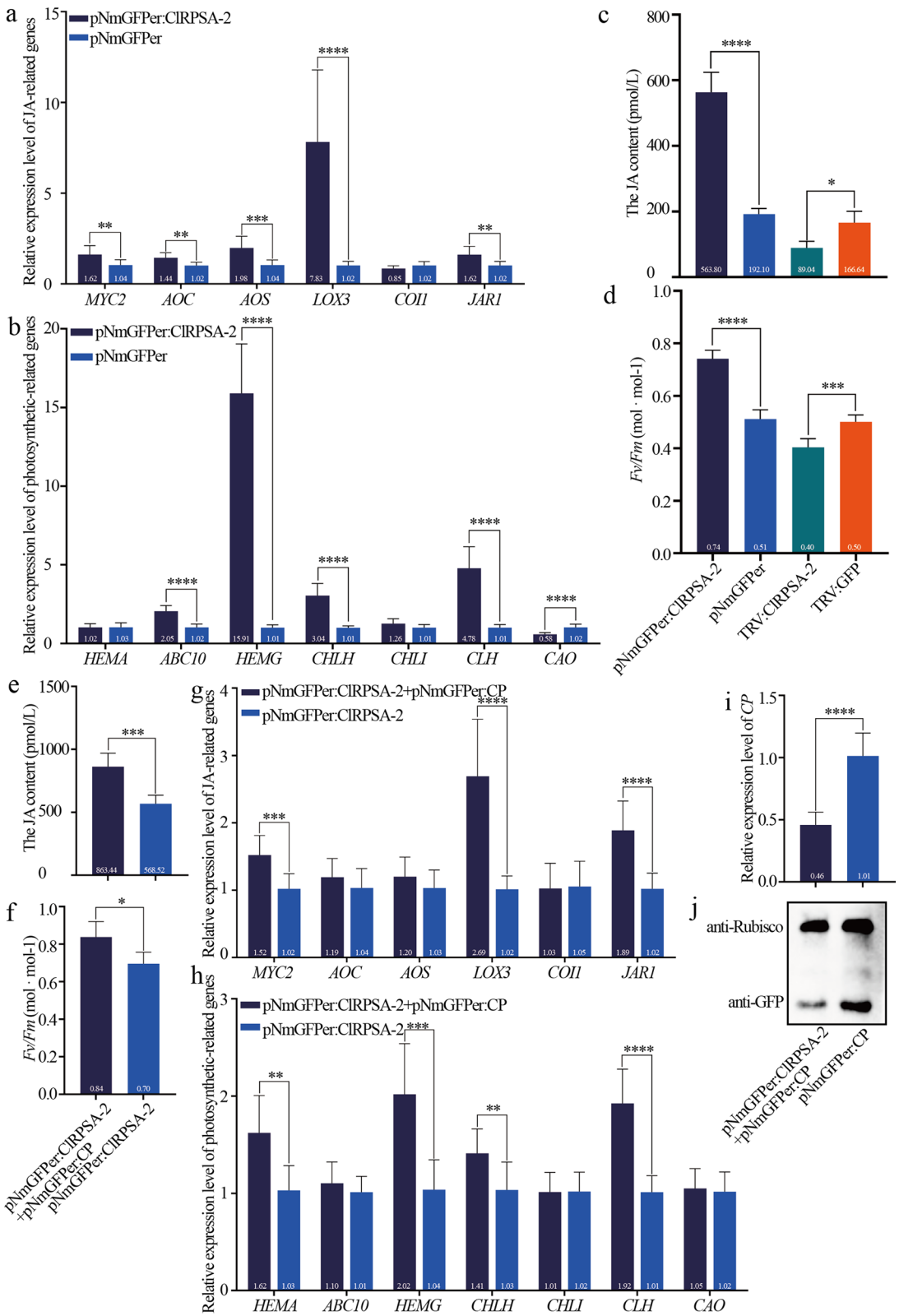

Fig. 5 (See legend on previous page.)

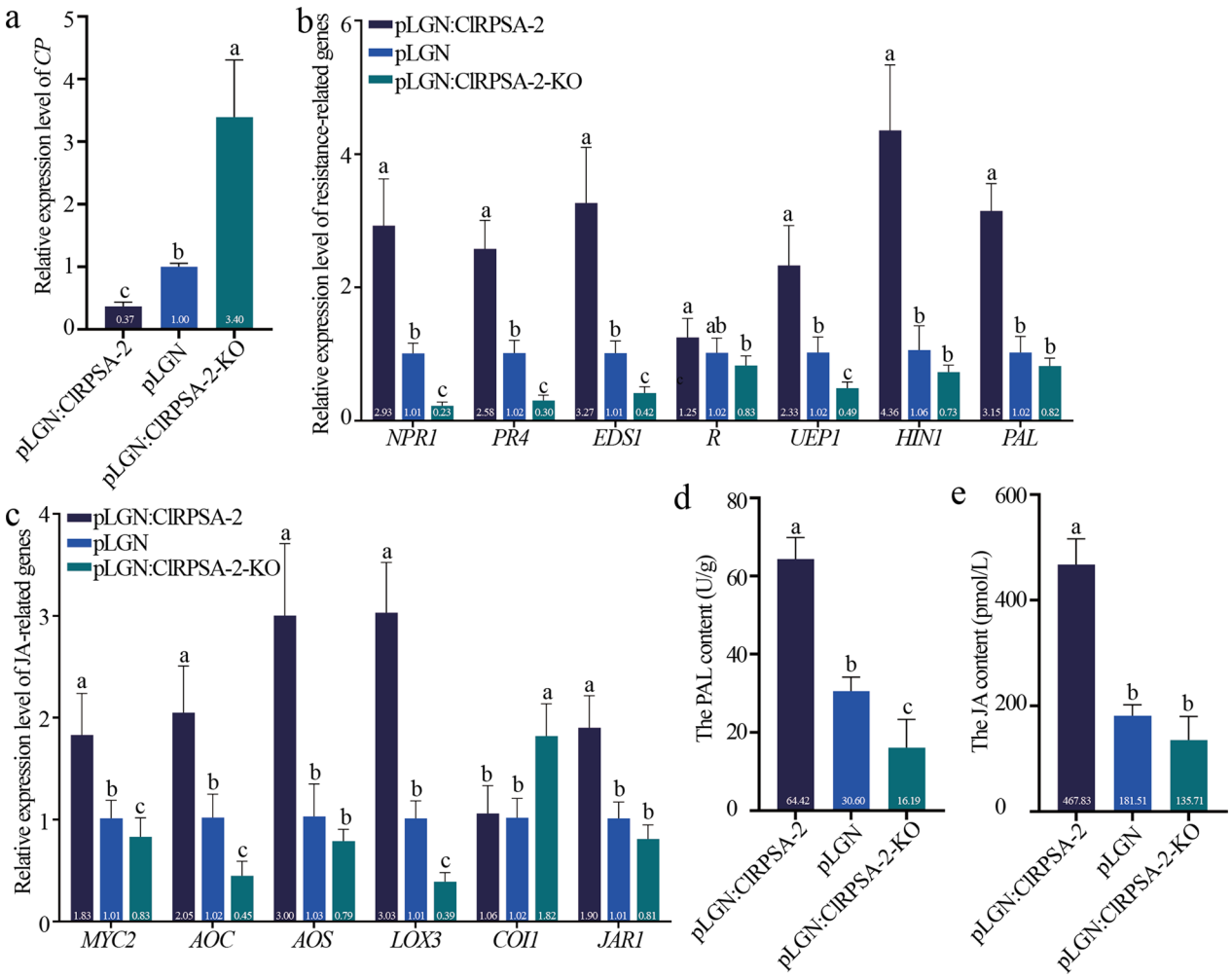

Fig. 6 *ClRPSA-2* positively regulates Eureka lemon anti-CYVCV defense. **a**–**c** The relative expression level of CYVCV *CP*, resistance-related genes, and jasmonic acid (JA)-related genes in *ClRPSA-2* transgenic hairy roots. *Actin* was an internal reference gene, one-way ANOVA test at 0.05 level ($n = 9$), data are mean ± SD. **d**, **e** The phenylalanine ammonia lyase and JA contents in *ClRPSA-2* transgenic hairy roots. One-way ANOVA test at 0.05 level ($n = 5$), data are mean ± SD

and 50.96%, respectively (Fig. 8). However, at 6 dpi, the CYVCV, CTV, CCDaV, and CTLV titers were 2.93-, 2.65-, 9.97-, and 1.69-fold that of the controls in *ClRPSA-2*-silenced CPV-, CTV-, CCDaV-, and CTLV-infected young Eureka lemon leaves (Fig. 8). These results indicated that ClRPSA-2 positively regulates a broad-spectrum resistance to citrus viruses.

Discussion

Because the viral genome is too small to encode all necessary proteins, virus-plant interactions are crucial for viral infection. Using the Eureka lemon cDNA library (Zeng et al. 2023), the 40S ribosomal protein, RPSA-2, was identified as a CYVCV-CP binding partner, indicating that ClRPSA-2 is involved in CYVCV infection modulation. Therefore, we aimed to characterize the regulatory role of ClRPSA-2 in citrus virus function in this study. ClRPSA-2 directly interacts with CP in the nucleus and membrane of *N. benthamiana* as a CYVCV resistance protein in Eureka lemon, and the N-terminal aas 22—122 acts as the binding region of ClRPSA-2 with CP and functions to inhibit CP expression.

Previous studies have shown that 40S RPs participate in the host's anti-viral immunity by interacting with viral proteins. Yang et al. (2021) suggested that CsRPS21 inhibits CCYV in *N. benthamiana* by interacting with CCYV P22. Wang et al. (2017) found that RPS11 interacts with the CMV LS2b protein and promotes CMV replication and accumulation. In addition,

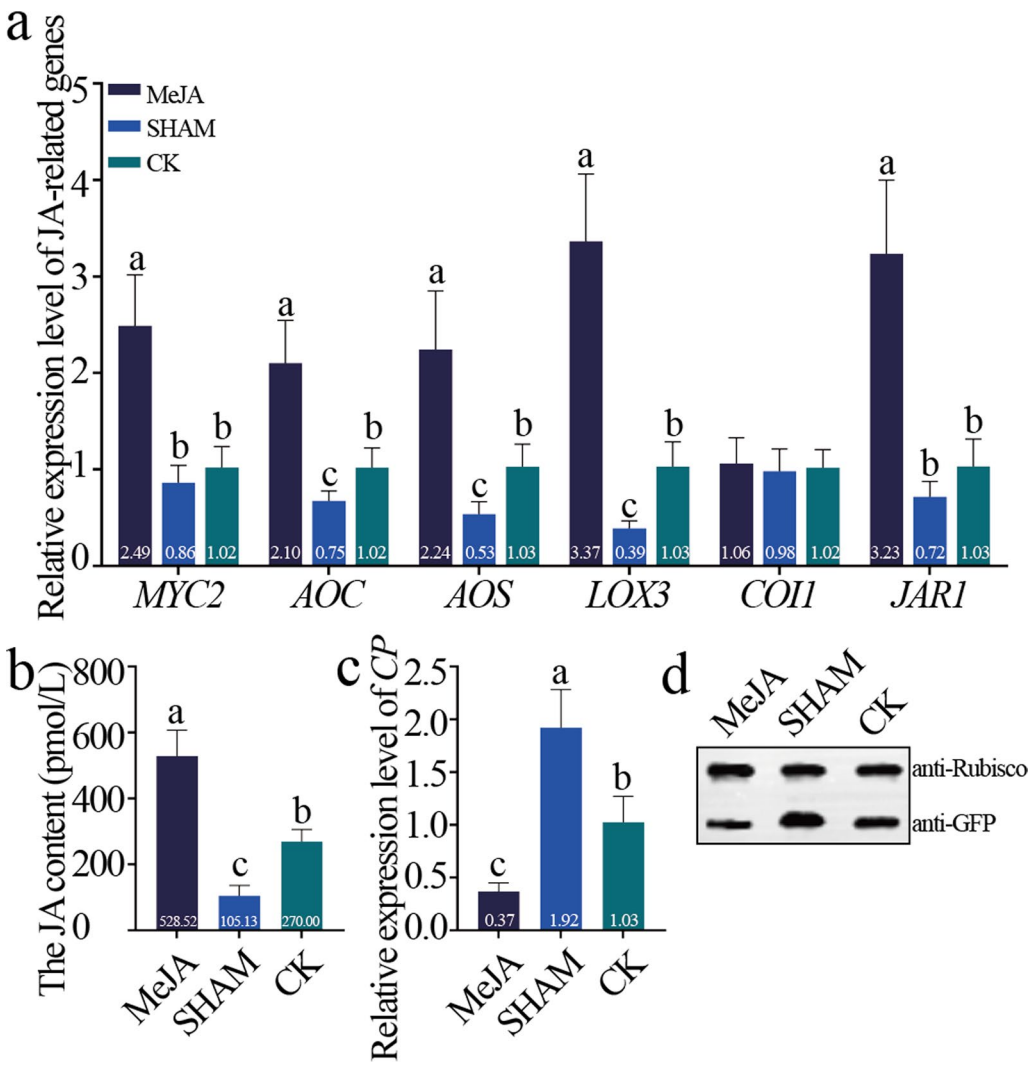

Fig. 7 Methyl jasmonate (MeJA) and JA inhibitor salicylhydroxamic acid (SHAM) treatment affect CYVCV accumulation through the JA signaling pathway. **a** Relative expression level of JA-related genes in MeJA and SHAM treatment virus-free Eureka lemon. *Actin* was an internal reference gene, determined by one-way ANOVA test at the 0.05 level ($n=9$). **b** The JA content in MeJA and SHAM treatment virus-free Eureka lemon. One-way ANOVA test at 0.05 level ($n=5$), data are mean ± SD. **c**, **d** The CYVCV titer was detected using real-time quantitative PCR analysis (RT-qPCR) and western blotting (WB) analysis. *Actin* was an internal reference gene, one-way ANOVA test at 0.05 level ($n=9$), data are mean ± SD; an anti-CYVCV CP antibody was used for WB analysis

the interaction between SMV 6K1 and GmRPS8 contributes to viral susceptibility (Hu et al. 2023).

RPSA, also known as p40 or RPS2, belongs to the laminin receptor family (DiGiacomo and Meruelo 2016). As a component of the 40S ribosome, RPSA was first isolated from rats (Tohgo et al. 1994). Subsequently, RPSA homologs were observed in amphibians, invertebrates, plants, yeasts, and bacteria (DiGiacomo and Meruelo 2016). The RPSA sequence is highly conserved and performs multiple functions; RPSA participates in the proliferation, invasion, and metastasis of tumors and regulates plant resistance to abiotic stresses (Ould-Abeih et al. 2012; Cloutier et al. 2022; Lu et al. 2023). Comparative proteomic analysis has shown that RPSA participates in nitrogen deficiency tolerance in cucumber fruit and in the tolerance of soybean seeds to flooding (Hao et al. 2021; Sharmin et al. 2021). *Capsicum annuum* RPSA-like CaSLP is a CaNAC035-interacting protein expressed in peppers that positively regulates the resistance of pepper to drought and *Pst.* DC3000 stress (Zhang et al. 2023). Recently, several studies have revealed the potential role of RPSA in plant disease. A previous study demonstrated that RPSA binds to tobacco etch potyvirus helper component-proteinase (HC-Pro) in aphid mouthparts and

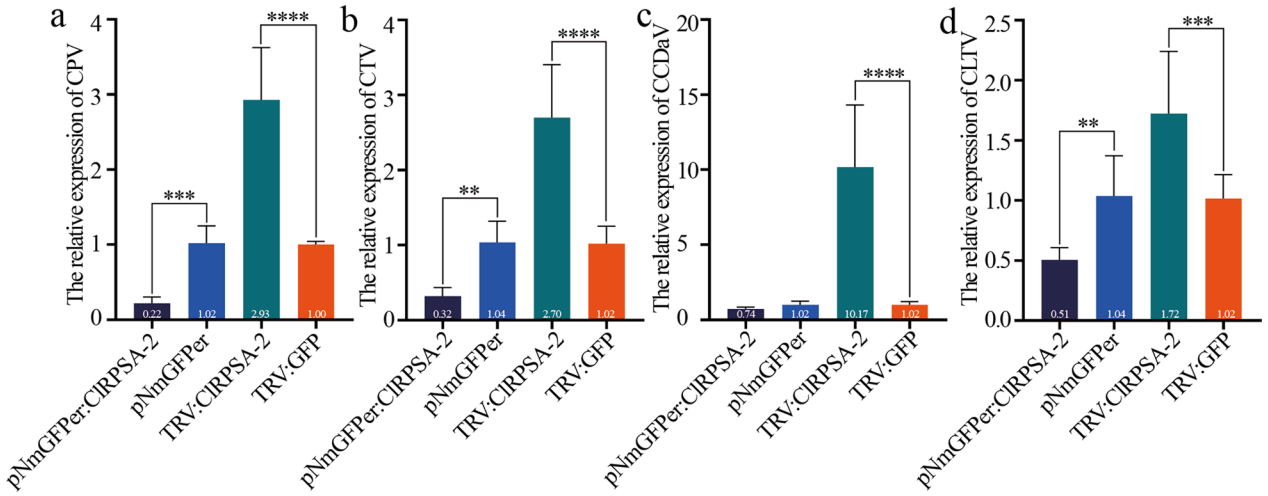

Fig. 8 ClRPSA-2 positively regulates a broad-spectrum resistance to citrus viruses. **a–d** The citrus psorosis virus, citrus tristeza virus, citrus chlorotic dwarf-associated virus, and citrus tatter-leaf virus titers were detected by real-time quantitative PCR analysis at 6 days post infiltration of pNmGFPer:ClRPSA-2 and TRV:ClRPSA-2. *Actin* was an internal reference gene, *t*-test, data are mean ± SD, n = 9, ** $P < 0.01$, *** $P < 0.001$, **** $P < 0.0001$

is involved in the virus transmission process (Fernández-Calvino et al. 2010). Based on protein–protein interactions (PPIs) and Y2H analyses, Kim et al. (2016) speculated that RPSA may be involved in the translation of tomato yellow leaf curl virus (TYLCV) proteins, providing favorable conditions for viral infection. In this study, ClRPSA-2 significantly inhibited CYVCV accumulation in Eureka lemon. To the best of our knowledge, this is the first study to show that RPSA is involved in plant antiviral responses. In addition, a previous study demonstrated that the CYVCV content was reduced in *ClRPS9-2* transgenic lemon plants (Zeng et al. 2023). However, no interaction between ClRPS9-2 and ClRPSA-2 was observed in the Y2H assay (Additional file 1: Figure S6). In the future, we should aim to elucidate whether ClRPS9-2 and ClRPSA-2 could synergistically inhibit CP accumulation.

Phytohormones, including JA, participate in the antiviral activity of plants. JA positively regulates plant resistance to the potato virus Y^{NTN} strain, CMV, and beet curly top virus (Petrovic et al. 1999; Lozano-Duran et al. 2011; Zhao et al. 2013). Furthermore, host proteins mediate plant resistance to viruses by increasing JA-mediated defense. For example, *SlMAPK3* enhances tomato tolerance to TYLCV, and *ZmGLK36* promotes maize resistance to maize rough dwarf virus and rice black-streaked dwarf virus by activating JA signaling (Li et al. 2017; Mahmood and Greenwood 2023). In this study, we demonstrated that ClRPSA-2 has three MYC binding sites, activates the expression of JA-related genes, and enhances the JA content, indicating that ClRPSA-2 may induce the immune response of Eureka lemon to CYVCV via the JA pathway; MeJA treatment reduced the CYVCV titer, while knockdown of the JA signaling pathway by SHAM treatment significantly increased the CYVCV titer. Moreover, ClRPSA-2 can enhance the resistance of Eureka lemon to CYVCV through the JA signaling pathway. Furthermore, MYB, MYC, ABRE, and G-box motifs were identified in ClRPSA-2; therefore, it would be interesting to determine the binding activity of ClRPSA-2 in specific DNA sequences.

An increasing number of reports highlight that improved photosynthetic efficiency can enhance plant resistance to virus infection (Zhou et al. 2017a; Bwalya et al. 2023). In addition, F_v/F_m reflects the potential maximum photosynthetic capacity of plants, which enhances the stress resistance of plants (Kim et al. 2019; Ren et al. 2024); it is also an important indicator for evaluating plant antiviral infection (Rys et al. 2014; Srilatha et al. 2019). In this study, we observed light responsiveness binding sites in ClRPSA-2, indicating that it may be involved in photosynthesis. Transient *ClRPSA-2* expression positively regulates photosynthesis-related gene expression, and F_v/F_m was 1.45-fold that of the control. These results indicate that the resistance factor ClRPSA-2 may also activate and enhance plant resistance to CYVCV via the photosynthetic pathway.

Conclusion

In this study, we demonstrated that the CYVCV-CP interacts with ClRPSA-2, and ClRPSA-2 negatively regulates CP expression in Eureka lemon. Our findings suggest that ClRPSA-2 suppresses the accumulation of CYVCV in lemons by activating the JA and photosynthetic signaling pathways, providing a new strategy for effective CYVCV control in China.

Methods

Plant materials and virus source

N. benthamiana, *N. tabacum*, virus-free Eureka lemon seedlings, and Eureka lemon seedlings inoculated with CYVCV, CPV, CTV, CCDaV, and CTLV were planted in a greenhouse at 25°C ± 3°C under a 16/8 h light/dark photoperiod. All primers used in this study are listed in Additional file 2: Table S4.

Characterization of ClRPSA-2

To characterize RPSA-2 from Eureka lemon, the full *ClRPSA-2* sequence was amplified using the specific primers (Additional file 2: Table S4), and the corresponding predicted aa sequence was analyzed as previously described by Zeng et al. (2023). Eighteen multiple-aligned homologous RPSA-2 sequences from *Citrus*, *Citrus*-related genera, and non-*Citrus* genera plants were obtained using DNAMAN V6 software. Phylogenetic analysis of these sequences was performed using the MEGA package and neighbor-joining method (Kumar et al., 2015). ClRPSA-2 binding sites were analyzed using plantCARE.

Vector construction

The homologous coding sequences (CDS) of *RPSA-2* from lemon (*ClRPSA-2*), sweet orange (*CsRPSA-2*), *Citrus clementina* (*CcRPSA-2*), *C. hongheensis* (*ChRPSA-2*), *N. tabacum* (*NtRPSA-2*), and four truncated mutants of *ClRPSA-2* were ligated into the vector pGADT7 (AD) (Puint, China) to generate the prey plasmids AD:ClRPSA-2, AD:CsRPSA-2, AD:CcRPSA-2, AD:ChRPSA-2, AD:NtRPSA-2, AD:ClRPSA-$2_{1—21}$ (aa residues 1—21), AD:ClRPSA-$2_{22—122}$ (aa residues 22—122), AD:ClRPSA-$2_{115—188}$ (aa residues 115—188), and AD:ClRPSA-$2_{189—316}$ (aa residues 189—316), respectively. The bait plasmid pGBKT7:CP (BD:CP) was constructed using a similar method (Zeng et al. 2023).

For the BiFC assays, the full-length CDS of *ClRPSA-2* and *CP* were cloned into the pSPYNE and pSPYCE (Puint, China) vectors to construct pSPYNE:ClRPSA-2 and pSPYCE:CP (Zhang et al. 2022), respectively.

For the LCI assay, *ClRPSA-2*, *CsRPSA-2*, *CcRPSA-2*, *ChRPSA-2*, and *NtRPSA-2* were cloned into PHNL-P14 to generate PHNL:ClRPSA-2, PHNL:CsRPSA-2, PHNL:CcRPSA-2, PHNL:ChRPSA-2, and PHNL:NtRPSA-2, respectively; *CP* was inserted into the PCCL:P9 vector to construct PCCL:CP (Yao et al. 2023).

For the Co-IP assays, pSPYCE:CP-GFP and pSPYCE:ClRPSA-2-His were constructed as previously described by Zeng et al. (2023).

For subcellular localization of ClRPSA-2 and co-localization of ClRPSA-2/CP in *N. benthamiana* leaf cells, the CDS of *ClRPSA-2* was fused with GFP and cloned into pCHF3 to obtain pCHF3:ClRPSA-2-GFP. In addition, a recombinant plasmid pCHF3:CP-mCherry fused with mCherry was constructed.

To transiently express *ClRPSA-2*, *CP*, and a serial of *ClRPSA-2* segments, the recombinant plasmids pNmGFPer:ClRPSA-2, pNmGFPer:CP, pNmGFPer:ClRPSA-$2_{1–21}$, pNmGFPer:ClRPSA-$2_{22–122}$, and pNmGFPer:ClRPSA-$2_{123–316}$ were constructed (Additional file 1: Figure S7). To silence *ClRPSA-2*, recombinant TRV vectors containing the 243 bp reverse complementary fragment of *ClRPSA-2* was prepared (Yang et al. 2023).

To establish a Eureka lemon hairy root transformation system over-expressing *ClRPSA-2*, the full-length CDS of *ClRPSA-2* was subcloned into a pLGN vector to obtain pLGN:ClRPSA-2 (Additional file 1: Figure S8). A 243-bp fragment of *ClRPSA-2* was reverse complementarily cloned into a pLGN vector to obtain the silencing recombinant plasmid pLGN:ClRPSA-2-KO (Xiao et al. 2023).

All recombinant plasmids were sequenced and verified before use. All of the primers used in this study are listed in Additional file 2: Table S4.

Identification of the interaction between ClRPSA-2 and CP

Y2H assay: The bait plasmid BD:CP and prey plasmids were used for a Y2H assay to verify the interaction between CP and RPSA-2 s. BD:CP and prey plasmids were co-transformed into the yeast strain Y2H Gold and applied to the SD/-Leu/-Trp selective medium. After 3–5 d of culture at 28°C, the positive clones were planted on the SD/-His/-Leu/-Trp/ABA/X-α-Gal and SD/-Ade/-His/-Leu/-Trp/ABA/X-α-Gal selective mediums as described by Zeng et al. (2023).

BiFC assay: pSPYNE:ClRPSA-2 and pSPYCE:CP were transformed into *Agrobacterium* EHA105. The *Agrobacterium* cultures containing pSPYNE:ClRPSA-2/pSPYCE:CP were co-infiltrated into *N. benthamiana* leaves. At 2 dpi, the infiltrated leaves were collected and observed using a FV3000 scanning confocal microscope (Olympus, Japan) (Zhou et al. 2017b).

LCI assay: The *Agrobacterium* strain EHA105 carrying PHNL:ClRPSA-2 and PCCL:CP was equally mixed and co-infiltrated into *N. benthamiana* leaves. At 2 dpi, the infiltrated leaves were used to observe the interaction between ClRPSA-2 and CP.

The Co-IP assay was used to verify the interaction between ClRPSA-2 and CP, as described by Liao et al. (2024).

The interactions between CP and ClRPSA-$2_{1–21}$, ClRPSA-$2_{22–122}$, ClRPSA-$2_{115–188}$, and ClRPSA-$2_{189–316}$ were preliminarily evaluated using the Y2H assay. BiFC and LCI were used to further verify the interaction between CP and ClRPSA-$2_{22–122}$.

Subcellular localization of ClRPSA-2

mCherry-PIP2A, mCherry-H2B, and mCherry-HDEL were agro-infiltrated with pCHF3:ClRPSA-2-GFP in *N. benthamiana* leaves to analyze the subcellular localization of ClRPSA-2. Additionally, *A. tumefaciens* cultures carrying pCHF3:ClRPSA-2-GFP and pCHF3:CP-mCherry were co-infiltrated into *N. benthamiana* leaves. The fluorescence signal in the infiltrated leaves was observed at 2 dpi (Varshney et al. 2023).

Effect of CP on the expression of *ClRPSA-2*

To determine whether *CP* expression affects the expression of *ClRPSA-2*, pNmGFPer:CP was agro-infiltrated into young Eureka lemon leaves, as described by Zeng et al. (2023). At 0, 3, 6, 9, and 12 dpi, the expression of *ClRPSA-2* was analyzed by RT-qPCR assay (Liu et al. 2023).

Effects of ClRPSA-2 on CP expression and citrus virus infection

To determine the function of ClRPSA-2 on CP expression, pNmGFPer:ClRPSA-2 was agro-infiltrated into Eureka lemon leaves. At 3 dpi, WB was used to analyze ClRPSA-2 expression, and at 0, 3, 6, 9, and 12 dpi, the expression of *ClRPSA-2* was analyzed by RT-qPCR. At 3 dpi, pNmGFPer:CP was re-infiltrated into the infiltrated leaves, and the CP expression was analyzed by WB and RT-qPCR assays at 0, 1, 3, 5, and 7 d after infiltration with pNmGFPer:CP. *ClRPSA-2* was silenced in Eureka lemon leaves by agro-infiltration of TRV2:ClRPSA-2 into young Eureka lemon leaves, as described above.

To determine the function of ClRPSA-2 in citrus virus infection, *ClRPSA-2* was transiently expressed and silenced in young CYVCV-, CPV-, CTV-, CCDaV-, and CTLV-infected Eureka lemon leaves, as described above, respectively. At 6 dpi, the infiltrated leaves were collected for an RT-qPCR assay.

Construction of Eureka lemon hairy root transformation system

To further explore the function of *ClRPSA-2*, pLGN:ClRPSA-2 and pLGN:ClRPSA-2-KO were used to establish an *A. rhizogenes*-mediated genetic transformation system, with *ClRPSA-2* over-expression and silencing, respectively, in the hairy roots of CYVCV-infected Eureka lemon (Xiao et al. 2023).

MeJA and JA inhibitors salicylhydroxamic acid treatment

The 0.1 mM MeJA and 0.2 mM salicylhydroxamic acid (SHAM) solution were prepared and sprayed onto virus-free and CYVCV-infected Eureka lemon plants (Nair et al. 2015; Hussain et al. 2021). Control plants were sprayed with 50% alcohol solution. Spraying was repeated on alternate days for a week. Fifteen days later, the samples were collected for RT-qPCR and WB assays, and the JA content was detected.

Physiological measurements

At 6 dpi, the *Fv*/*Fm* in Eureka lemon leaves with transiently expressed or silenced *ClRPSA-2* was tested as previously described by Xiong et al. (2023). The JA and PAL contents in *ClRPSA-2* transiently expressed or silenced Eureka lemon leaves, transformed hairy root, and MeJA and SHAM treated samples were determined using the corresponding ELISA detection kits (Sinobestbio, China).

Statistical analysis

The results were statistically analyzed using GraphPad Prism 9.3.1 software (Anwar et al. 2024). Differences between two groups were analyzed using a Student *t*-test, and the data are presented as mean ± standard deviation (SD), $^{*}P < 0.05$, $^{**}P < 0.01$, $^{***}P < 0.001$, $^{****}P < 0.0001$. Differences among three or more groups were analyzed using a one-way analysis of variance test; the data are presented as mean ± SD, and different lower case letters represent differences at the $P < 0.05$ level. We used n = 9 for RT-qPCR analysis and n = 5 for JA and PAL content detection. A normal distribution and homogeneity of variance test were performed before analysis; a Wilcoxon test was used for a non-normal distribution, and a Welch correction was performed when the variance was not uniform.

Abbreviations

aa	Amino acids
BiFC	Bimolecular fluorescence complementation
CCDaV	Citrus chlorotic dwarf-associated virus
CCYV	Cucurbit chlorotic yellows virus
ClRPSA-2	Eureka lemon 40S RPSA
CMV	Cucumber mosaic virus
Co-IP	Co-immunoprecipitation
CP	Coat protein
CPV	Citrus psorosis virus
CTLV	Citrus tatter-leaf virus
CTV	Citrus tristeza virus
CYVCV	Citrus yellow vein clearing virus
Fv/Fm	Maximum photochemical efficiency
JA	Jasmonic acid
LCI	Luciferase complementation imaging
PAL	Phenylalanine ammonia lyase
RPs	Ribosomal proteins
RT-qPCR	Real-time quantitative PCR
SHAM	Salicylhydroxamic acid
SMV	Soybean mosaic virus
TRV	Tobacco rattle virus
TYLCV	Tomato yellow leaf curl virus
WB	Western blotting
Y2H	Yeast two hybrid

Supplementary Information

The online version contains supplementary material available at https://doi.org/10.1186/s42483-024-00301-5.

Additional file 1: Figure S1. Characterization of CIRPSA-2. **Figure S2.** *CP* promotes the expression of *CIRPSA-2* in Eureka lemon. **Figure S3.** The silence of *CIRPSA-2* enhances CP expression. **Figure S4.** CIRPSA-2 mediates the expression of resistance-related genes and enhances phenylalanine ammonia lyase (PAL) content. **Figure S5.** Jasmonic acid- and photosynthetic-related genes were down-regulated in *CIRPSA-2*-silenced Eureka lemon leaves. **Figure S6.** The yeast-two hybrid (Y2H) assay showed that CIRPSA-2 can not interact with CIRPS9-2. **Figure S7.** The pNmGFPer construct. **Figure S8.** The pLGN construct.

Additional file 2: Table S1. Pairwise alignment of RPSA-2 protein sequences. **Table S2.** CIRPSA-2 binding sites were analyzed using PlantCARE. **Table S3.** The Eureka lemon CIRPSA-2 hairy root transformation system. **Table S4.** Primers used in this study.

Acknowledgements
We sincerely thank Prof. Jianmin Zhou (University of Chinese Academy of Sciences, Beijing, China) for providing PHNL-P14 and PCCL-P9 plasmids and Prof. Xiuping Zou (Southwest University, Chongqing, China) for providing pLGN and pNmGFPer plasmids.

Author contributions
PL, YZ, and BL designed the experiments. PL, MH, DD, and XD performed the experiments. PL and LC analyzed the data. PL wrote the manuscript. PL, YZ, and BL revised and polished the manuscript. All authors contributed to the article and approved the submitted version.

Funding
This research was financially supported by Natural Science Foundation of Chongqing (CSTB2024NSCQ-MSX0311), Agricultural Technology Research and Development Service Program of Wanzhou District, and the Opening Project of Guangxi Key Laboratory of Germplasm Innovation and Utilization of Specialty Commercial Crops in North Guangxi (GASCKF202404).

Availability of data and materials
All data generated or analyzed during this study are included in this published article and its supplementary information files.

Declarations

Ethics approval and consent to participate
Not applicable.

Consent for publication
Not applicable.

Competing interests
The authors declare that they have no competing interests.

Received: 5 June 2024 Accepted: 16 December 2024
Published online: 11 February 2025

References

Abrahamian P, Tian TY, Posis K, Guo Y, Yu D, Blomquist CL, et al. Genetic analysis of the emerging citrus yellow vein clearing virus reveals a divergent virus population in American isolates. Plant Dis. 2024;108(6):1544–54. https://doi.org/10.1094/PDIS-09-23-1963-RE.

Anwar H, Azer A, AboElHassan RG. Influence of a specially designed geometric device and modified scan bodies on the accuracy of a maxillary complete arch digital implant scan: an in vitro study. J Prosthet Dent. 2024;131(4):683.e1-7. https://doi.org/10.1016/j.prosdent.2024.02.020.

Bin Y, Xu JJ, Duan Y, Ma ZM, Zhang Q, Wang CQ, et al. The titer of citrus yellow vein clearing virus is positively associated with the severity of symptoms in infected citrus seedlings. Plant Dis. 2022;106(3):828–34. https://doi.org/10.1094/PDIS-02-21-0232-RE.

Bwalya J, Widyasari K, Völz R, Kim KH. Chloroplast-related host proteins interact with NIb and NIa-Pro of soybeans mosaic virus and induce resistance in the susceptible cultivar. Virus Res. 2023;336: 199205. https://doi.org/10.1016/j.virusres.2023.199205.

Chang IF, Szick-Miranda K, Pan SQ, Bailey-Serres J. Proteomic characterization of evolutionarily conserved and variable proteins of *Arabidopsis* cytosolic ribosomes. Plant Physiol. 2005;137(3):848–62. https://doi.org/10.1104/pp.104.053637.

Cloutier G, Khalfaoui T, Beaulieu J. A58 characterization of the 37/67 kDa laminin receptor in colorectal cancer cells. J Canadian Assoc Gastroenterol. 2022;5(1):67–8. https://doi.org/10.1093/jcag/gwab049.057.

DiGiacomo V, Meruelo D. Looking into laminin receptor: critical discussion regarding the non-integrin 37/67-kDa laminin receptor/RPSA protein. Biol Rev Camb Philos Soc. 2016;91(2):288–310. https://doi.org/10.1111/brv.12170.

Fatehullah A, Doherty C, Pivato G, Allen G, Devine L, Nelson J, et al. Interactions of the 67 kDa laminin receptor and its precursor with laminin. Biosci Rep. 2010;30(2):73–9. https://doi.org/10.1042/BSR20090023.

Fernández-Calvino L, Goytia E, López-Abella D, Giner A, Urizarna M, Vilaplana L, et al. The helper-component protease transmission factor of tobacco etch potyvirus binds specifically to an aphid ribosomal protein homologous to the laminin receptor precursor. J Gen Virol. 2010;91(11):2862–73. https://doi.org/10.1099/vir.0.022335-0.

Hao J, Li Q, Yu HJ, Wang H, Chai L, Miao TT, et al. Comparative proteomic analysis of cucumber fruits under nitrogen deficiency at the fruiting stage. Hortic Plant J. 2021;7(1):59–72. https://doi.org/10.1016/j.hpj.2020.12.002.

Helderman TA, Deurhof L, Bertran A, Richard MMS, Kormelink R, Prins M, et al. Members of the ribosomal protein S6 (RPS6) family act as pro-viral factor for tomato spotted wilt orthotospovirus infectivity in *Nicotiana benthamiana*. Mol Plant Pathol. 2022;23(3):431–46. https://doi.org/10.1111/mpp.13169.

Hu T, Guo DQ, Li BW, Wang LQ, Liu H, Yin JL, et al. Soybean 40S ribosomal protein S8 (GmRPS8) interacts with 6K1 protein and contributes to soybean susceptibility to soybean mosaic virus. Viruses. 2023;15(12):2362. https://doi.org/10.3390/v15122362.

Hussain A, Noman A, Arif M, Farooq S, Khan MI, Cheng P, et al. A basic helix-loop-helix transcription factor *CabHLH113* positively regulate pepper immunity against *Ralstonia solanacearum*. Microb Pathog. 2021;156:104909. https://doi.org/10.1016/j.micpath.2021.104909.

Kim N, Kim J, Bang B, Kim I, Lee HH, Park J, et al. Comparative analyses of tomato yellow leaf curl virus C4 protein-interacting host proteins in healthy and infected tomato tissues. The Plant Pathol J. 2016;32(5):377–87. https://doi.org/10.5423/PPJ.FT.08.2016.0165.

Kim JH, Bhandari SR, Chae SY, Cho MC, Lee JG. Application of maximum quantum yield, a parameter of chlorophyll fluorescence, for early determination of bacterial wilt in tomato seedlings. Hortic Environ Biotechnol. 2019;60(6):821–9. https://doi.org/10.1007/s13580-019-00182-0.

Kumar D, Haq I, Chapagai D, Tripathi D, Donald D, Hossain M, et al. Hormone signaling: current perspectives on the roles of salicylic acid and its derivatives in plants. The Form Struct Activity Phytochem Recent Adv Phytochem. 2015;45:115–36. https://doi.org/10.1007/978-3-319-20397-3_5.

Li YZ, Qin L, Zhao JJ, Muhammad T, Cao HH, Li HL, et al. *SlMAPK3* enhances tolerance to tomato yellow leaf curl virus (TYLCV) by regulating salicylic acid and jasmonic acid signaling in tomato (*Solanum lycopersicum*). PLoS ONE. 2017;12(2): e0172466. https://doi.org/10.1371/journal.pone.0172466.

Liao P, Zeng T, Huangfu MY, Zheng CR, Ren JQ, Zhou CY, et al. Eureka lemon zinc finger protein CIDOF3.4 interacts with citrus yellow vein clearing virus coat protein to inhibit viral infection1. J Integr Agric. 2024;23(6):1979–93. https://doi.org/10.1016/j.jia.2024.03.049.

Liu YJ, Wang YL, Wang Q, Zhang YH, Shen WX, Li RH, et al. Development of a sensitive and reliable reverse transcription droplet digital PCR assay for the detection of citrus yellow vein clearing virus. Adv Virol. 2019;164(3):691–7. https://doi.org/10.1007/s00705-018-04123-7.

Liu CH, Liu H, Hurst J, Timko MP, Zhou CY. Recent advances on citrus yellow vein clearing virus in citrus. Hortic Plant J. 2020;6(4):216–22. https://doi.org/10.1016/j.hpj.2020.05.001.

Liu H, Du BY, Ma XC, Wang Y, Cheng NN, Zhang YH. Overexpression of major latex protein 423 (*NtMLP*423) enhances the chilling stress tolerance

in *Nicotiana tabacum*. Plant Sci. 2023;329: 111604. https://doi.org/10.1016/j.plantsci.2023.111604.
Lozano-Durán R, Rosas-Díaz T, Gusmaroli G, Luna AP, Taconnat L, Deng XW, et al. Geminiviruses subvert ubiquitination by altering CSN-mediated derubylation of SCF E3 ligase complexes and inhibit jasmonate signaling in *Arabidopsis thaliana*. Plant Cell. 2011;23(3):1014–32. https://doi.org/10.1105/tpc.110.080267.
Lu YW, Wang SZ, Jiao YS. The effects of deregulated ribosomal biogenesis in cancer. Biomolecules. 2023;13(11):1593. https://doi.org/10.3390/biom13111593.
Maghsoudi R, Nassrollahnejad S, Aghajanzadeh S, Hashemian BSM. Transmissibility of citrus yellow vein clearing virus by three dominant citrus aphids. Iranian J Plant Protect Sci. 2023;54(1):101–13. https://doi.org/10.22059/ijpps.2023.353042.1007016.
Mahmood MA, Greenwood JR. *ZmGLK36* transcription factor bestows viral resistance in rice and wheat. Trends Plant Sci. 2023;29(6):613–5. https://doi.org/10.1016/j.tplants.2023.12.007.
Malygin AA, Bondarenko EI, Ivanisenko VA, Protopopova EV, Karpova GG, Loktev VB. C-terminal fragment of human laminin-binding protein contains a receptor domain for venezuelan equine encephalitis and tick-borne encephalitis viruses. Biochem Mosc. 2009;74(12):1328–36. https://doi.org/10.1134/S0006297909120050.
Meena RP, Baranwal VK. Genetic diversity of the coat protein gene and biological variation of citrus yellow vein clearing virus infecting different citrus species. Tropical Plant Pathol. 2020;45(5):467–75. https://doi.org/10.1007/s40858-020-00333-0.
Nair A, Kolet SP, Thulasiram HV, Bhargava S. Role of methyl jasmonate in the expression of mycorrhizal induced resistance against *Fusarium oxysporum* in tomato plants. Physiol Mol Plant Pathol. 2015;92:139–45. https://doi.org/10.1016/j.pmpp.2015.10.002.
Ould-Abeih MB, Petit-Topin I, Zidane N, Baron B, Bedouelle H. Multiple folding states and disorder of ribosomal protein SA, a membrane receptor for laminin, anticarcinogens, and pathogens. Biochemistry. 2012;51(24):4807–21. https://doi.org/10.1021/bi300335r.
Petrovic N, Miersch O, Ravnikar M, Kovac M. Relation between the endogenous jasmonic acid and decreased potato virus Y^{NTN} concentration in potato treated with jasmonic acid. Phyton-Annales Rei Botanicae. 1999;39(3):249–52. https://doi.org/10.3171/2023.8.PEDS23348.
Rajamäki ML, Xi DH, Sikorskaite-Gudziuniene S, Valkonen JPT, Whitham SA. Differential requirement of the ribosomal protein S6 and ribosomal protein S6 kinase for plant-virus accumulation and interaction of S6 kinase with potyviral VPg. Mol Plant Microbe Interact. 2017;30(5):374–84. https://doi.org/10.1094/MPMI-06-16-0122-R.
Ren HZ, Yu YT, Huang C, Li DY, Ni JL, Lv WY, et al. Genome-wide identification and characterization of tea SGR family members reveal their potential roles in chlorophyll degradation and stress tolerance. Agronomy-Basel. 2024;14(4):769. https://doi.org/10.3390/agronomy14040769.
Rys M, Juhász C, Surówka E, Janeczko A, Saja D, Tóbiás I, et al. Comparison of a compatible and an incompatible pepper-tobamovirus interaction by biochemical and non-invasive techniques: chlorophyll a fluorescence, isothermal calorimetry and FT-Raman spectroscopy. Plant Physiol Biochem. 2014;83:267–78. https://doi.org/10.1016/j.plaphy.2014.08.013.
Sharmin RA, Karikari B, Chang FG, Al Amin GM, Bhuiyan MR, Hina A, et al. Genome-wide association study uncovers major genetic loci associated with seed flooding tolerance in soybean. BMC Plant Biol. 2021;21(1):497. https://doi.org/10.1186/s12870-021-03268-z.
Srilatha P, Yousuf F, Methre R, Vishnukiran T, Agarwal S, Poli Y, et al. Physical interaction of RTBV ORFI with D1 protein of *Oryza sativa* and Fe/Zn homeostasis play a key role in symptoms development during rice tungro disease to facilitate the insect mediated virus transmission. Virology. 2019;526:117–24. https://doi.org/10.1016/j.virol.2018.10.012.
Sun YD, Yokomi R. Genotype sequencing and phylogenetic analysis revealed the origins of citrus yellow vein clearing virus California isolates. Viruses. 2024;16(2):188. https://doi.org/10.3390/v16020188.
Tio PH, Jong WW, Cardosa MJ. Two dimensional VOPBA reveals laminin receptor (LAMR1) interaction with dengue virus serotypes 1, 2 and 3. Virology J. 2005;2:25. https://doi.org/10.1186/1743-422X-2-25.
Tohgo A, Takasawa S, Munakata H, Yonekura H, Hayashi N, Okamoto H. Structural determination and characterization of a 40 kDa protein isolated from rat 40 S ribosomal subunit. FEBS Lett. 1994;340(1–2):133–8. https://doi.org/10.1016/0014-5793(94)80188-6.
Varshney V, Hazra A, Rao V, Ghosh S, Kamble NU, Achary RK, et al. The *Arabidopsis* F-box protein SKP1-INTERACTING PARTNER 31 modulates seed maturation and seed vigor by targeting JASMONATE ZIM DOMAIN proteins independently of jasmonic acid-isoleucine. Plant Cell. 2023;35(10):3712–38. https://doi.org/10.1093/plcell/koad199.
Wang RL, Du ZY, Bai ZQ, Liang ZS. The interaction between endogenous 30S ribosomal subunit protein S11 and cucumber mosaic virus LS2b protein affects viral replication, infection and gene silencing suppressor activity. PLoS ONE. 2017;12(8): e0182459. https://doi.org/10.1371/journal.pone.0182459.
Wang CQ, Zhang Q, Li JX, Wang XL, Li CX, Bin Y, et al. The coat protein of citrus yellow vein clearing virus directly targets the ascorbate peroxidase 1 in lemon (ClAPX1) to facilitate virus accumulation. Front Plant Sci. 2023;14:1306580. https://doi.org/10.3389/fpls.2023.1306580.
Xiao YX, Dutt M, Ma HJ, Xiao C, Tong Z, Wang ZQ, et al. Establishment of an efficient root mediated genetic transformation method for gene function verification in citrus. Sci Hortic. 2023;321: 112298. https://doi.org/10.1016/j.scienta.2023.112298.
Xiong W, Lan T, Mo BX. Extraribosomal functions of cytosolic ribosomal proteins in plants. Front Plant Sci. 2021;12: 607157. https://doi.org/10.3389/fpls.2021.607157.
Xiong B, Li L, Li Q, Mao HQ, Wang LXY, Bie YH, et al. Identification of photosynthesis characteristics and chlorophyll metabolism in leaves of citrus cultivar (*Harumi*) with varying degrees of chlorosis. Int J Mol Sci. 2023;24(9):8394. https://doi.org/10.3390/ijms24098394.
Yang X, Wei Y, Shi YJ, Han XY, Chen SY, Yang LL, et al. Cucumber ribosomal protein CsRPS21 interacts with P22 protein of cucurbit chlorotic yellows virus. Front Microbiol. 2021;12: 654697. https://doi.org/10.3389/fmicb.2021.654697.
Yang X, Wang Y, Liu TX, Liu Q, Liu J, Lü TF, et al. *CYCLOIDEA*-like genes control floral symmetry, floral orientation, and nectar guide patterning. Plant Cell. 2023;35(8):2799–820. https://doi.org/10.1093/plcell/koad115.
Yao J, Zhang SL, Wu N, Li XM, Ahmad B, Wu JY, et al. KNOX transcription factor VvHB63 affects grape seed development by interacting with protein VvHB06. Plant Sci. 2023;330: 111665. https://doi.org/10.1016/j.plantsci.2023.111665.
Zeng T, Liao P, Zheng CR, Gao HX, Ye X, Zhou CY, et al. The interaction between the lemon ribosomal protein CIRPS9-2 and citrus yellow vein clearing virus coat protein affects viral infection and gene silencing suppressor activity. Mol Plant Pathol. 2023;24(9):1047–62. https://doi.org/10.1111/mpp.13347.
Zhang YH, Liu CH, Wang Q, Wang YL, Zhou CY, Zhou Y. Identification of *Dialeurodes citri* as a vector of citrus yellow vein clearing virus in China. Plant Dis. 2019a;103(1):65–8. https://doi.org/10.1094/PDIS-05-18-0911-RE.
Zhang YH, Liu YJ, Wang YL, Wang Q, He SG, Li XY, et al. Transmissibility of citrus yellow vein clearing virus by contaminated tools. J Plant Pathol. 2019b;101(1):169–71. https://doi.org/10.1007/s42161-018-0141-8.
Zhang LN, Wang LT, Chen X, Zhao LJ, Liu XY, Wang YH, et al. The protein phosphatase 2C clade a TaPP2CA interact with calcium-dependent protein kinases, TaCDPK5/TaCDPK9–1, that phosphorylate TabZIP60 transcription factor from wheat (*Triticum aestivum* L.). Plant Sci. 2022;321:111304. https://doi.org/10.1016/j.plantsci.2022.111304.
Zhang HF, Pei YP, He Q, Zhu W, Jahangir M, Haq SU, et al. Salicylic acid-related ribosomal protein CaSLP improves drought and *Pst*. DC3000 tolerance in pepper. Mol Hortic. 2023. https://doi.org/10.1186/s43897-023-00054-3.
Zhao PP, Shang J, Guo ZC, Xie HF, Xi DH, Sun X, et al. Temperature-related effects of treatments with jasmonic and salicylic acids on *Arabidopsis* infected with cucumber mosaic virus. Russ J Plant Physiol. 2013;60(5):672–80. https://doi.org/10.1134/S1021443713050166.
Zhou ML, Zhang KX, Sun ZM, Yan ML, Chen C, Zhang XQ, et al. LNK1 and LNK2 co-repressors interact with the MYB3 transcription factor in phenylpropanoid biosynthesis. Plant Physiol. 2017a;174(3):1348–58. https://doi.org/10.1104/pp.17.00160.
Zhou X, Zhu T, Zhu LS, Luo SS, Deng XG, Lin HH, et al. The role of photoreceptors in response to cucumber mosaic virus in *Arabidopsis thaliana*. J Plant Growth Regul. 2017b;36(2):257–70. https://doi.org/10.1007/s00344-016-9635-9.